**Supporting information for**

# A two-pronged strategy to alleviate tumor hypoxia and potentiate photodynamic therapy by mild hyperthermia

Zhijie Zhang[a,#], Zibing Wang[a,#], Yuxuan Xiong[a,#], Chong Wang[a], Qingyuan Deng[a], Tian Yang[a], Qingqing Xu[a], Zhengtao Yong[a], Xiangliang Yang[a, b, c, d, e, f], and Zifu Li[a, c, d, e, f, *]

[a] National Engineering Research Center for Nanomedicine, College of Life Science and Technology, Huazhong University of Science and Technology, Wuhan, 430074, P. R. China

[b] GBA Research Innovation Institute for Nanotechnology, Guangdong, 510530, P. R. China

[c] Key Laboratory of Molecular Biophysics of Ministry of Education, College of Life Science and Technology, Huazhong University of Science and Technology, Wuhan, 430074, P. R. China

[d] Hubei Bioinformatics and Molecular Imaging Key Laboratory, College of Life Science and Technology, Huazhong University of Science and Technology, Wuhan, 430074, P. R. China

[e] Hubei Key Laboratory of Bioinorganic Chemistry and Materia Medical, Huazhong University of Science and Technology, Wuhan, 430074, P. R. China

[f] Hubei Engineering Research Center for Biomaterials and Medical Protective Materials, Huazhong University of Science and Technology, Wuhan, 430074, P. R. China

# These authors contribute equally.

* Address correspondence to:

Zifu Li, Ph.D., Professor

Huazhong University of Science and Technology

1037 Luoyu Road, Wuhan, 430074, P. R. China

E-mail: zifuli@hust.edu.cn

**Experimental Section:**

**Materials and Reagents.** Chlorin e6 (Ce6, 98%) and 1,3-diphenylisobenzofuran (DPBF, 97%) were purchased from J&K Scientific Ltd (Beijing, China). Polyvinylpyrrolidone (PVP-K30, Mw: 49000) was purchased from Aladdin Reagent Inc. (Shanghai, China). Ferricyanide ($K_3[Fe(CN)_6]\cdot 3H_2O$) and Tris(4,7-diphenyl-1,10-phenanthroline)ruthenium(II) dichloride complex ($[Ru(dpp)_3]Cl_2$) were purchased from Macklin Biochemical Co., Ltd (Shanghai, China). Dimethyl sulfoxide (DMSO), methanol, ethanol, hydrochloric acid, tween-80 and hydrogen peroxide ($H_2O_2$) were purchased from Sinopharm Chemical Reagent Co.Ltd, (Shanghai, China). Phosphate buffer saline (PBS), trypsin, RPMI 1640 medium, fetal bovine serum (FBS) and 4',6-diamidino-2-phenylindole (DAPI) were purchased from Gibco BRL/Life Technologies (Grand Island, USA). Dichloro-dihydro-fluorescein diacetate (DCFH-DA) and 4% Paraformaldehyde Fix Solution were purchased from Beyotime. Calcein-AM/PI double stain kit and Annexin V-FITC/PI Apoptosis Detection Kit were purchased from Yeasen Biotechnology Co., Ltd (Shanghai, China). Thiazolyl blue tetrazolium bromide (MTT) was purchased from Solarbio Science & Technology Co., Ltd (Beijing, China).

**Synthesis of PB, HPMB and Ce6@HMPB.** 282.85 mg $K_3[Fe(CN)_6]\cdot 3H_2O$ and 10 g PVP-K30 were dissolved in hydrochloric acid (0.01 M) by stirring for 0.5 h at room temperature. Then, the mixture was heated at 80 °C for 20 h without stirring to form cubic PB NPs. PB NPs were washed with ethanol and ultrapure water for 3 times by ultracentrifugation (12000 rpm, 20 min). HMPB NPs were made by chemical etching of PB NPs. 60 mg PB NPs and 300 mg PVP-K30 were dissolved in hydrochloric acid (1 M) and stirred for 2 h at room temperature. The mixture was then sealed in a Teflon-lined autoclave and kept at 140 °C for 4 h. HMPB NPs were washed with ethanol and ultrapure water for 3 times by ultracentrifugation (12000 rpm, 20 min). For loading of Ce6, 1 mg Ce6 dissolved in 1 mL methanol was mixed with 10 mg HMPB NPs dissolved in 9 mL ultrapure water. The mixture was stirred overnight at room temperature and then centrifugated to remove unloaded Ce6. The Ce6 encapsulation efficiency of Ce6@HMPB NPs was calculated as follows:

$$\text{Ce6 encapsulation efficiency} = \frac{\text{feeding amount of Ce6 - amount of Ce6 in supernatant}}{\text{feeding amount of Ce6}} \times 100\%$$

**Instruments.** The hydrodynamic diameter and Zeta-potential profiles were acquired on a dynamic laser light scattering instrument (DLS, Zetasizer Nano ZS90, Malvern, UK). The morphology of NPs was characterized by transmission electron microscopy (TEM, HT7700 HITACHI Co., Japan, accelerating voltage: 120 kV). The absorption spectra were collected using a UV-Vis spectrophotometer (Lambda 35, PerkinElmer Instruments Co., Ltd., Shanghai, China). Single point fluorescence of Ce6 and Ce6@HMPB NPs was recorded by Fluro Max+ spectrometer (Horiba, Japan). The cellular behavior was observed using Confocal laser scanning microscope (CLSM, Olympus, FV3000). Pore-size distribution of HMPB NPs was measured by a Physisorption Analyzer (ASAP2420-4MP) through the nitrogen ($N_2$) adsorption-desorption isothermal method.

**Cell lines and animals.** 4T1 cancer cells and HUVECs were purchased from BeNa Culture Collection, China. The cells were cultured in RPMI 1640 medium supplemented with 10% fetal bovine serum (FBS) and 1% penicillin/streptomycin under humidified conditions with 5% $CO_2$ and 37 °C. BALB/c (female, SPF, 5 weeks) were purchased from Beijing Vital River Laboratory Animal Technology Co. Ltd. All animal handing procedures were performed in accordance with the internationally accepted principles and Guidelines for the Care and Use of Laboratory Animals of Huazhong University of Science and Technology. Experimental protocols were approved by the Institutional Animal Ethical Committee of the Huazhong University of Science and Technology. The mice were kept in specific pathogen-free environment, and had access to food and water ad libitum.

**Stability test.** The stability of Ce6@HMPB NPs was evaluated by monitoring size changes of Ce6@HMPB NPs in different media including ultrapure water, PBS buffer (0.01 M, pH 7.4) and 50% (v/v) FBS for a week.

**Measurement of photothermal performance.** The temperature of PB, HMPB and Ce6@HMPB NPs dispersion under 808 nm laser irradiation (1 W/cm$^2$, 50 μg/mL) was monitored by FLIR E50 Infrared (IR) camera (FLIR Systems Inc., Wilsonville, OR, USA). To study the effect of concentration on temperature elevation, different concentrations of Ce6@HMPB NPs solutions (0-0.2 mg/mL) were prepared, and irradiated by 808 nm laser irradiation (1 W/cm$^2$) for 10 min. To study the effect of laser power on temperature elevation, Ce6@HMPB NPs solution was irradiated by 808 nm laser with different powers

(0.5, 1 and 1.5 W/cm$^2$). The photothermal stability of Ce6@HMPB NPs was also tested by recording four cycles of heating and cooling period. The temperature of the solutions was monitored by a thermal imager, and recorded every 30 seconds. The photothermal conversion efficiencies (η) of PB, HMPB and Ce6@HMPB NPs were calculated according to previous literature[1].

**Evaluation of catalase activity by oxygen probe.** To evaluate the catalase activity of PB, HMPB and Ce6@HMPB NPs, NPs were respectively added in 96-well plate (final concentration fixed to 20 μg/mL) with 10 μL 10 μg/mL oxygen probe ($[Ru(dpp)_3)]Cl_2$) and 2% (v/v) $H_2O_2$. After incubation for 10 min at 25 °C, the fluorescence intensity of wells was measured by FlexStation 3 Multi-Mode Microplate Reader ($\lambda_{ex}$=488 nm, $\lambda_{em}$=620 nm). To evaluate the effect of Ce6@HMPB NPs concentration on $O_2$ generation, $H_2O_2$, different amount of Ce6@HMPB NPs and 10 μL $[Ru(dpp)_3)]Cl_2$ were respectively added in 96-well plate to make final concentration of Ce6@HMPB NPs at 80, 40, 20, 10 and 0 μg/mL. After incubation for 10 min at 25 °C, the fluorescence intensity of wells was measured by FlexStation 3 Multi-Mode Microplate Reader ($\lambda_{ex}$=488 nm, $\lambda_{em}$=620 nm). To evaluate the effect of $H_2O_2$ concentration on $O_2$ generation, different amount of $H_2O_2$, Ce6@HMPB NPs and 10 μL $[Ru(dpp)_3)]Cl_2$ were respectively added in 96-well plate to make final concentration of $H_2O_2$ at 8%, 4%, 2% and 0 v/v. After incubation for 10 min at 25 °C, the fluorescence intensity of wells was measured. To evaluate the effect of temperature on catalase activity, $H_2O_2$, Ce6@HMPB NPs and $[Ru(dpp)_3)]Cl_2$ were respectively added in centrifuge tubes (total volume fixed to 3 mL) to make final concentration of $H_2O_2$ and Ce6@HMPB NPs at $1\times10^{-4}$ M and 3 μg/mL. After incubation for 5 min at 25 °C, 37 °C and 45 °C, the fluorescence intensity of each group was measured by FlexStation 3 Multi-Mode Microplate Reader ($\lambda_{ex}$=488 nm, $\lambda_{em}$=620 nm).

**Bubble generation experiment.** 12 mL 100 μg/mL PB, HMPB or Ce6@HMPB NPs dispersion was added with 4 mL $H_2O_2$ and 14 mL ultrapure water to make the final concentration of nanoparticles and $H_2O_2$ to 40 μg/mL and 4% v/v. Then let these liquids stand for 60 min. Pictures were taken in 0, 10, 20, 30 and 60 min.

**Detection of $^1O_2$ production.** 1 mg of DPBF was dissolved in 1 mL of ethanol to obtain the stock solution of DPBF (1 mg/mL). Then, 50 μL of DPBF solution was added into 1950

μL of Ce6@HMPB NPs solutions (2 μg/mL as Ce6) with or without $H_2O_2$. Then, the mixtures were irradiated with a 660 nm laser (200 mW/cm$^2$) or an 808 nm laser (1.5 W/cm$^2$) plus 660 nm laser (200 mW/cm$^2$) for 2, 4 and 6 min. The decay of absorbance of DPBF at 426 nm with time represents ROS generation capacity.

**Cellular uptake.** The cellular uptake behavior was carried out using flow cytometry and confocal laser scanning microscope (CLSM, Olympus, FV3000). 4T1 cancer cells were seeded in 12-well plate at a density of 1.5×10$^5$ cells and cultured for 24 h. Then, the supernatant was removed and 4T1 cancer cells were incubated with free Ce6 and Ce6@HMPB NPs (4 and 8 μg/mL as Ce6) for 6 h. The supernatant was then removed, and cells were washed with PBS for three times, then digested by 200 μL trypsin. The digested cells were collected by centrifugation (1500 rpm, 5 min). The intracellular Ce6 was detected by flow cytometry in APC channel. For CLSM observation, 4T1 cancer cells were seeded in confocal dishes at a density of 1×10$^5$ cells and cultured for 24 h. Then, the supernatant was removed and 4T1 cancer cells were incubated with free Ce6 and Ce6@HMPB NPs (1 and 2 μg/mL as Ce6) for 6 h. The supernatant was then removed, and cells were washed with PBS for three times, then fixed by paraformaldehyde and stained with 5 μg/mL DAPI for 20 min. After being washed with PBS for three times, the cells were observed by CLSM. The excitation wavelengths of DAPI and Ce6 were 358 nm and 405 nm, respectively.

**Intracellular ROS generation.** The intracellular ROS generation was detected by flow cytometry. 4T1 cancer cells were seeded in 12-well plate at a density of 1.5×10$^5$ cells and cultured for 24 h. Then, the supernatant was removed and 4T1 cancer cells were incubated with free Ce6 and Ce6@HMPB NPs (4 and 8 μg/mL as Ce6) for 6 h. The supernatant was then removed and cells were washed with PBS for three times and supplemented with 1 mL DCFH-DA (10 μg/mL). After incubated for 20 min, cells in Ce6+660 nm group and Ce6@HMPB+660 nm group were irradiated with 200 mW/cm$^2$ 660 nm laser for 2 min. Cells in Ce6@HMPB+808 nm+660 nm group were irradiated with 1 W/cm$^2$ 808 nm laser for 5 min and then irradiated with 200 mW/cm$^2$ 660 nm laser for 2 min. The cells were digested and collected by centrifugation. The intracellular ROS was detected by flow cytometry in FITC channel.

***In vitro* cytotoxicity study.** *In vitro* cytotoxicity was studied by MTT assay. 4T1 cancer cells were seeded in 96-well plates at a density of $1\times10^4$ cells and incubated for 24 h. Then, the cells were incubated with Ce6 and Ce6@HMPB NPs solutions (0, 0.25, 0.5, 1, 2 and 8 μg/mL as Ce6) for 6 h. The medium containing Ce6 and Ce6@HMPB NPs was then replaced with fresh medium. Cells in Ce6+660 nm and Ce6@HMPB+660 nm group were irradiated with 660 nm laser at 200 mW/cm$^2$ for 2 min. Cells in Ce6@HMPB+808 nm and Ce6@HMPB+808 nm+660 nm group were irradiated with 1 W/cm$^2$ 808 nm laser for 5 min and then irradiated with 200 mW/cm$^2$ 660 nm laser for 2 min. 24 h later, 10 μL of MTT (5 mg/mL) was added to each well and cultured for 4 h. Finally, the medium was replaced with 150 μL of DMSO to dissolve the formazan. The cell viability was calculated using the absorbance at 492 nm measured by microplate reader (Thermo, Multi Skan).

To determine the dark toxicity of Ce6, HMPB NPs, and Ce6@HMPB NPs, 4T1 and HUVEC cells were incubated with Ce6 (0, 1, 2, 4, 8 and 16 μg/mL), HMPB NPs (0, 10, 20, 40, 80 and 160 μg/mL), and Ce6@HMPB NPs (containing 0, 1, 2, 4, 8 and 16 μg/mL Ce6) without laser irradiation. 24 h later, 10 μL of MTT (5 mg/mL) was added to each well and cultured for 4 h. Finally, the medium was replaced with 150 μL of DMSO to dissolve the formazan. The cell viability was calculated using the absorbance at 492 nm.

**Live/dead staining.** 4T1 cancer cells were seeded in confocal dishes ($1\times10^5$ cells per well) and incubated for 24 h. Then, the medium was discarded and replenished with fresh medium containing Ce6 and Ce6@HMPB NPs (the Ce6 concentration was 2 μg/mL). 6 h after, the cells were washed with PBS for three times and added with 1 mL medium. Then, cells in Ce6+660 nm group and Ce6@HMPB+660 nm group were irradiated with 660 nm laser (200 mW/cm$^2$) for 2min. Cells in Ce6@HMPB+808 nm+660 nm group were irradiated with 808 nm laser (1 W/cm$^2$) for 5 min and then irradiated with 660 nm laser (200 mW/cm$^2$) for 2 min. 2 h after, cells were stained with Calcein-AM/PI for CLSM observation.

**Cell apoptosis assay**. Annexin V-FITC/PI apoptosis kit was used to detect the cell apoptosis. 4T1 cancer cells were seeded in 12-well plates and incubated for 12 h. Then the cells were exposed to different treatments including PBS, Ce6@HMPB, Ce6@HMPB+2 min 660 nm laser irradiation and Ce6@HMPB+5 min 808 nm laser irradiation+2 min 660 nm laser irradiation (in an equivalent Ce6 amount of 2 μg/mL). After

2 h, the cells were harvested and stained with Annexin V-FITC and PI, subsequently analyzed by flow cytometry.

**Tumor models.** Subcutaneous 4T1 tumor model was established by subcutaneous injection of 4T1 cancer cells ($1\times10^6$ cells in 100 μL sterile PBS) into the right flank of the BALB/c mice. The tumor growth was monitored daily. For constructing 4T1 orthotopic tumor model, the skin located in the right fourth abdomen of mice was cut by surgery, and then injected with single-cell suspension of $5 \times 10^5$ 4T1 cancer cells per mouse on the abdomen adipose pad. The tumorous growth was monitored daily. The length (L) and width (W) of tumors were measured with a vernier caliper, and then the tumor volume (V) was calculated by the following formula: $V= L\times W^2/2$.

**Pharmacokinetic study.** Subcutaneous 4T1 tumor model (n=3) was employed to study pharmacokinetic of Ce6@HMPB NPs. Ce6@HMPB NPs were systematically injected via tail vein. At various time points (0.25 h, 0.5 h, 1 h, 2 h, 6 h, 12 h, 24 h and 48 h), the blood samples (10 μL) were extracted and digested. The concentration of Cu in each sample was measured by ICP-OES.

***In vivo* and *ex vivo* biodistribution of Ce6 and Ce6@HMPB NPs.** The biodistribution of Ce6 and Ce6@HMPB NPs was investigated in 4T1 subcutaneous tumor model. When tumor volume reached 200 $mm^3$, mice were intravenously injected with Ce6 or Ce6@HMPB NPs (5 mg/kg Ce6). The *in vivo* fluorescence of Ce6 and Ce6@HMPB NPs was imaged by a Xenogen IVIS *in vivo* imaging system at different time points. To determine the accumulation and localization of Ce6 in tumors and various organs, mice were sacrificed 12- and 24-hour post-injection while tumor, heart, liver, spleen, lung, and kidneys were harvested for *ex vivo* imaging using a Xenogen IVIS imaging system.

***In vivo* photothermal imaging.** To evaluate photothermal performance of Ce6@HMPB NPs *in vivo*, the 4T1 subcutaneous-bearing mice were injected with Ce6@HMPB NPs (5 mg/kg Ce6, 100 μL). At 12 h post injection, the mice were anesthetized and the tumor areas were exposed to 808 nm laser (0, 1, 1.5 and 1.75 $W/cm^2$) for 10 min. The real-time temperature was monitored every 30 seconds using an infrared camera.

**Analysis of extracellular matrix related proteins and cancer associated fibroblasts.** When tumor volume of 4T1 orthotopic tumor reached 300 $mm^3$, the mice were randomly

divided into saline, Ce6@HMPB and Ce6@HMPB+808 nm laser group. Saline and Ce6@HMPB (5 mg/kg Ce6) were i.v. administered. After 12 h, mice in Ce6@HMPB+808 nm laser group were treated with 808 nm laser for 10 min with the temperature of tumors limited to 43-45 °C. After 12 h, the tumors were harvested, fixed, and embedded in paraffin, and sections with 10 μm thickness were prepared. For analysis of extracellular matrix related proteins, MASSON staining, collagen I (Abcam: ab270993), fibronectin (Abcam: ab268020) immunofluorescent staining were conducted. For analysis of cancer associated fibroblasts (CAFs), α-SMA (Affinity, AF1032) immunofluorescent staining were conducted.

**Evaluation of solid stress.** When tumor volume of 4T1 orthotopic tumor reached 300 $mm^3$, the mice were randomly divided into saline, Ce6@HMPB and Ce6@HMPB+808 nm laser group. Saline and Ce6@HMPB NPs (5 mg/kg Ce6) were i.v. administered. After 12 h, mice in Ce6@HMPB+808 nm laser group were treated with 808 nm laser for 10 min with the temperature of tumors limited to 43-45 °C. After 12 h, the tumors were harvested and cut from the surface to 80% depth. After relaxing for 10 min in PBS, the tumor opening length was measured[2]. The normalized tumor solid stress was calculated by the following equation: Normalized solid stress=tumor opening length/tumor height.

**Evaluation of tumor vasculature.** When tumor volume of 4T1 orthotopic tumor reached 300 $mm^3$, the mice were randomly divided into saline, Ce6@HMPB and Ce6@HMPB+808 nm laser group. Saline and Ce6@HMPB NPs (5 mg/kg Ce6) were i.v. administered. After 12 h, mice in Ce6@HMPB+808 nm laser group were treated with 808 nm laser for 10 min with the temperature of tumors limited to 43-45 °C. After 12 h, the tumors were harvested, fixed, and embedded in paraffin, and sections with 10 μm thickness were prepared. The tumor vessels were evaluated by CD31 (Abcam, ab182981) immunofluorescent staining.

**Detection of tumor hypoxia.** When tumor volume of 4T1 orthotopic tumor reached 300 $mm^3$, the mice were randomly divided into saline, Ce6@HMPB and Ce6@HMPB+808 nm laser group. Saline and Ce6@HMPB NPs (5 mg/kg Ce6) were i.v. administered. After 12 h, mice in Ce6@HMPB+808 nm laser group were treated with 808 nm laser for 10 min with the temperature of tumors limited to 43-45 °C. After 2 h, the tumors were harvested, fixed, and embedded in paraffin, and sections with 10 μm thickness were prepared. The tumor

hypoxia was evaluated by HIF-1α (PTG, 20960-1-AP) immunofluorescent staining.

***In vivo* antitumor effect.** Subcutaneous 4T1 tumors-bearing mice were divided randomly to six groups when tumor volume reached 200 $mm^3$ (day 0): Saline, Ce6+660 nm laser, Ce6@HMPB, Ce6@HMPB+808 nm laser, Ce6@HMPB+660 nm laser and Ce6@HMPB+808 nm+660 nm laser. In day 0, saline, Ce6 and Ce6@HMPB NPs (5 mg/kg Ce6) were i.v. administered. After 12 h, mice in Ce6@HMPB+808 nm laser group and Ce6@HMPB+808 nm+660 nm laser group were treated with 808 nm laser for 10 min with the temperature of tumors limited to 43-45 °C. After 2 h, mice in Ce6+660 nm laser, Ce6@HMPB+660 nm laser and Ce6@HMPB+808 nm+660 nm laser group were treated with 660 nm laser (200 $mW/cm^2$) for 10 min. The length (L) and width (W) of tumors were measured with a vernier caliper every two days, and then the tumor volume (V) was calculated by the following formula: $V= L\times W^2/2$. Relative tumor volume was calculated by the dividing tumor volume by the tumor volume in day 0. The weight of mice was also monitored every two days. At day 14, the experimental mice were euthanized and the tumors were gathered, photographed, and weighted. The tumor inhibition rate for each group was calculated using the following equation: inhibition ratio=(Wc–We)/Wc×100%, where Wc represents the tumor weight of the blank group and We represents the tumor weight of the experimental group. The therapeutic effect was also evaluated by histological assay. Excised tumors were fixed, embedded, and then submitted to Hematoxylin and Eosin (H&E), Ki67, and Caspase 3 staining.

**Statistical analysis.** All the data in the present study were processed and presented as mean ± standard deviation (SD). The semi-quantitative analysis of fluorescence intensity was conducted with image J 1.53c. The statistical significances between two groups were assessed with Student's t-test. One-way ANOVA test was performed for comparison of multiple groups. All statistical calculations were conducted on GraphPad Prism 8.0. P values: * indicated $P<0.05$; ** indicated $P<0.01$; *** indicated $P<0.001$; **** indicated $P<0.0001$; ns indicated not significant.

**Supplementary Figures**

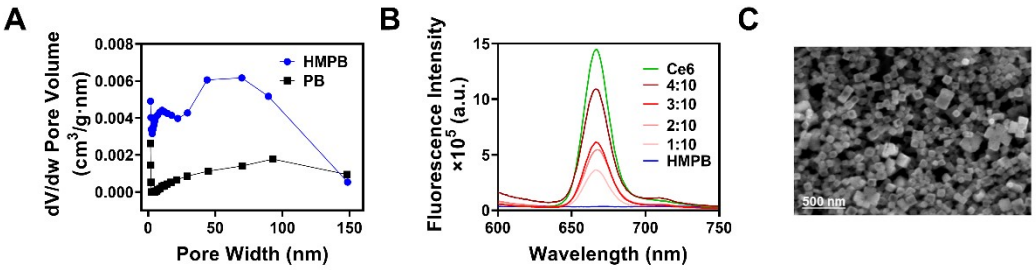


Figure S1. (A) Pore-size distribution of PB and HMPB NPs. (B) Fluorescence intensity of Ce6, HMPB NPs and Ce6@HMPB NPs in DMSO with different feeding amount ratio of Ce6 and HMPB NPs from 1:10 to 4:10. (C) SEM image of Ce6@HMPB NPs. The scale bar is 500 nm.

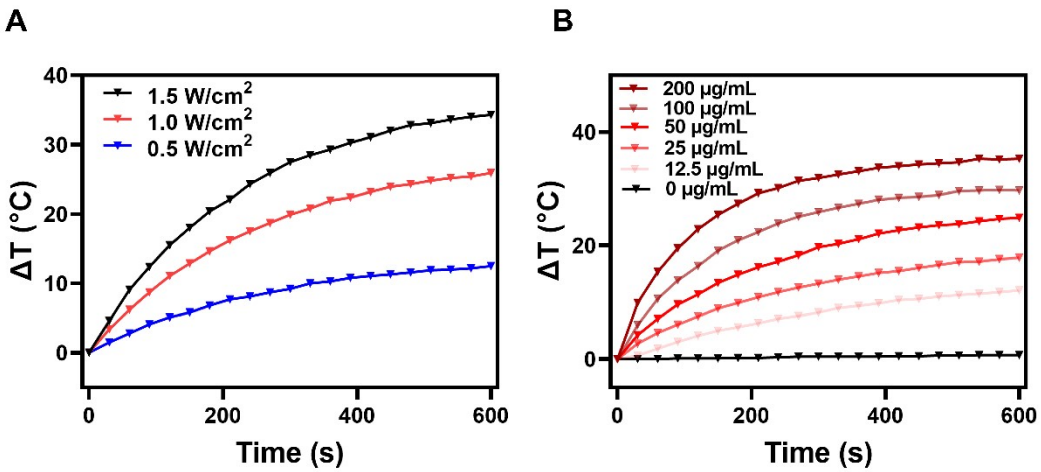


Figure S2. (A) Temperature changes of Ce6@HMPB dispersion (50 μg/mL) under 808 nm laser irradiation with different power. (B) Temperature changes of Ce6@HMPB dispersion with different concentration under 1.0 W/cm$^2$ 808 nm laser irradiation.

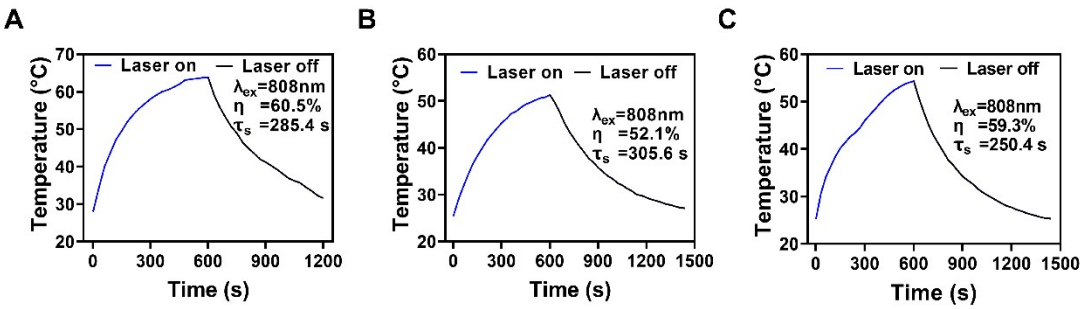


Figure S3. Temperature changes of PB (A), HMPB (B) and Ce6@HMPB NPs (C) dispersions (50 μg/mL) with 808 nm laser on for 10 min and then off.

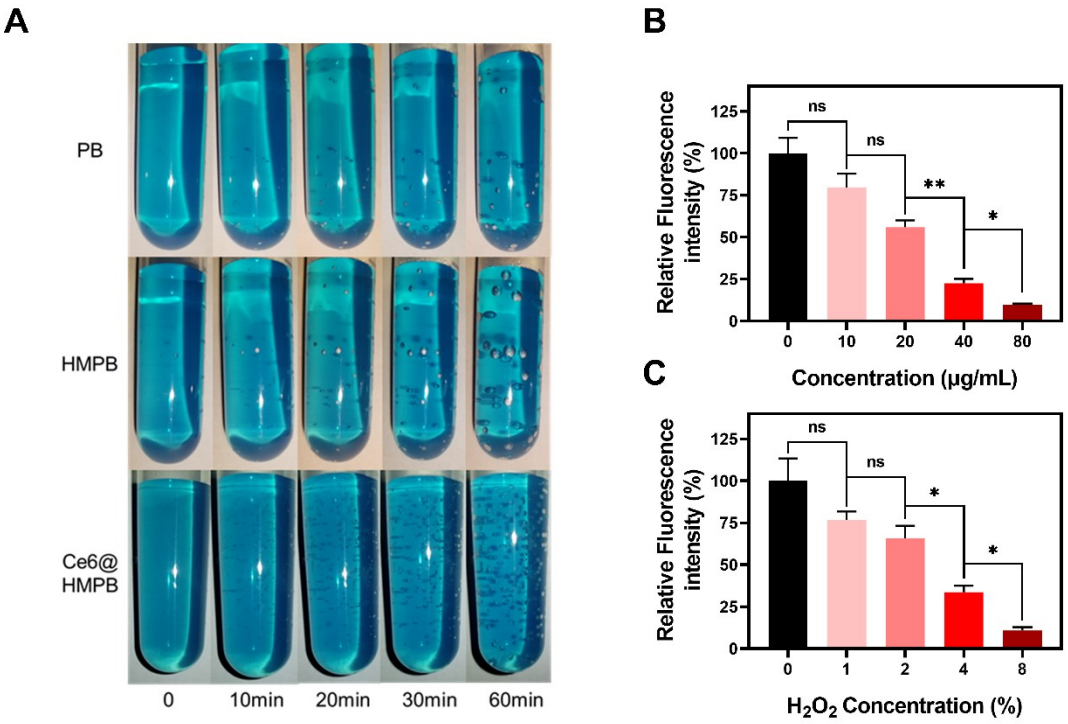


Figure S4. (A) Bubble generation with time in $H_2O_2$ solution with different nanoparticles. Relative fluorescence of $O_2$ probe $[Ru(dpp)_3]Cl_2$ in 4% v/v $H_2O_2$ solution containing different concentration of Ce6@HMPB NPs (B) and in different concentration of $H_2O_2$ solution containing 20 μg/mL Ce6@HMPB NPs (C). Error bar indicates SD (n=3). *, $P<0.05$, **, $P<0.01$ by Student's t-test, ns stands for not significant.

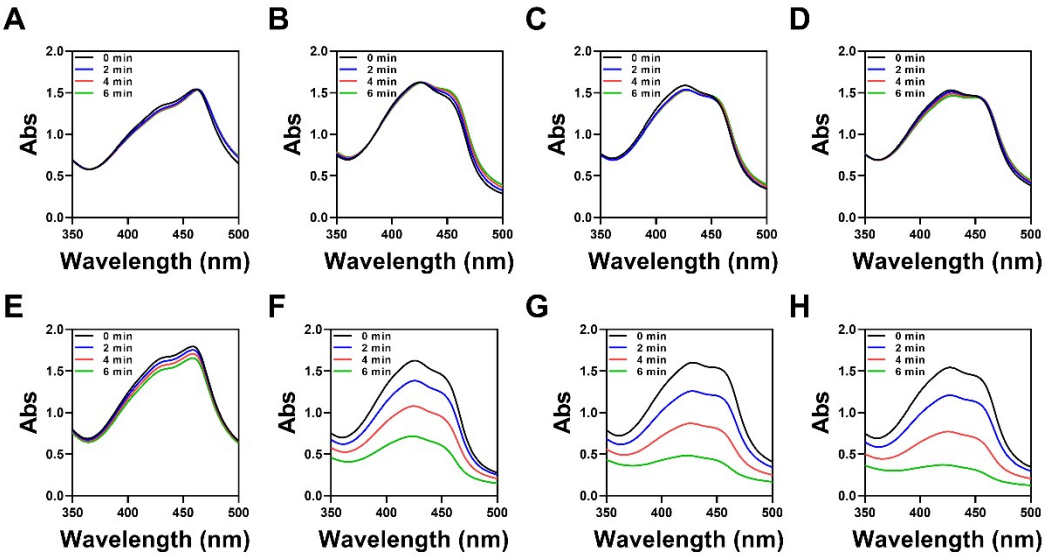


Figure S5. The UV-vis absorbance of DPBF solution in different groups at different time point. A: DPBF, B: DPBF+Ce6@HMPB NPs, C: DPBF+Ce6@HMPB NPs+$H_2O_2$, D: DPBF+Ce6@HMPB NPs+$H_2O_2$+808 nm (1.5 W/cm$^2$), E: DPBF+660 nm (200 mW/cm$^2$), F: DPBF+Ce6@HMPB NPs+660 nm, G: DPBF+Ce6@HMPB NPs+$H_2O_2$+660 nm, H: DPBF+Ce6@HMPB NPs+$H_2O_2$+808 nm+660 nm.

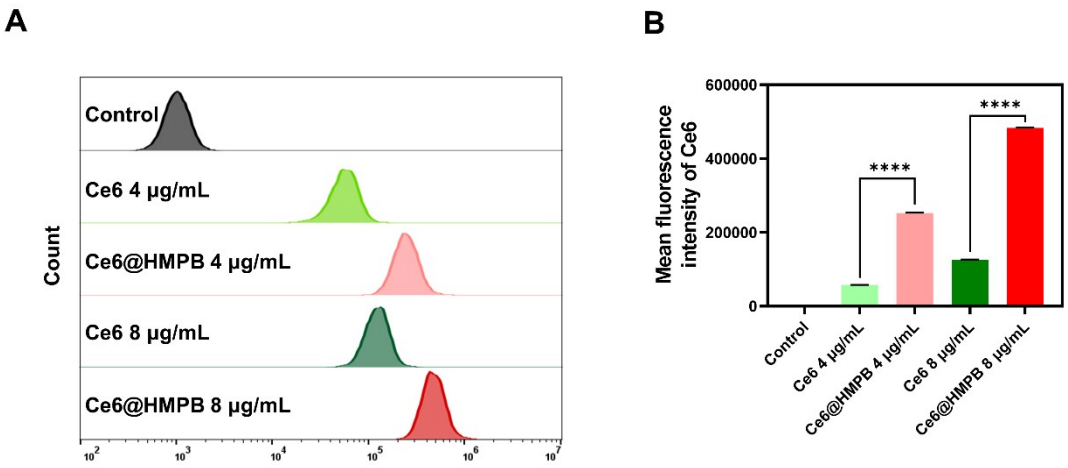


Figure S6. Flowcytometry analysis (A) and quantification (B) of intracellular Ce6 fluorescence after 6 h incubation with Ce6 or Ce6@HMPB NPs. Error bar indicates SD (n=3). ****, P<0.0001 by Student's t-test.

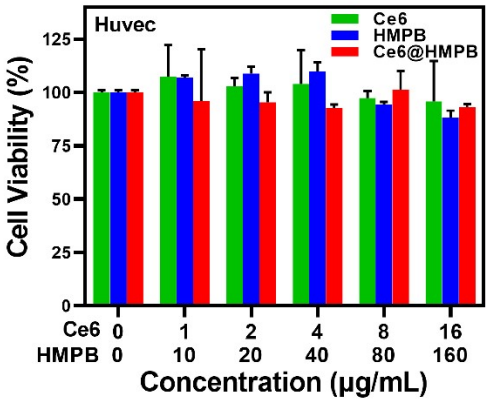


Figure S7. Dark cytotoxicity of Ce6, HMPB NPs and Ce6@HMPB NPs to Huvec cells. Error bar indicates SD (n=3).

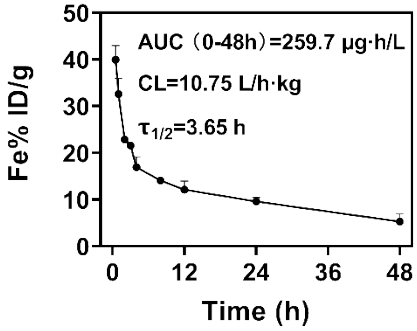


Figure S8. Pharmacokinetics of Ce6@HMPB NPs determined by ICP-OES.

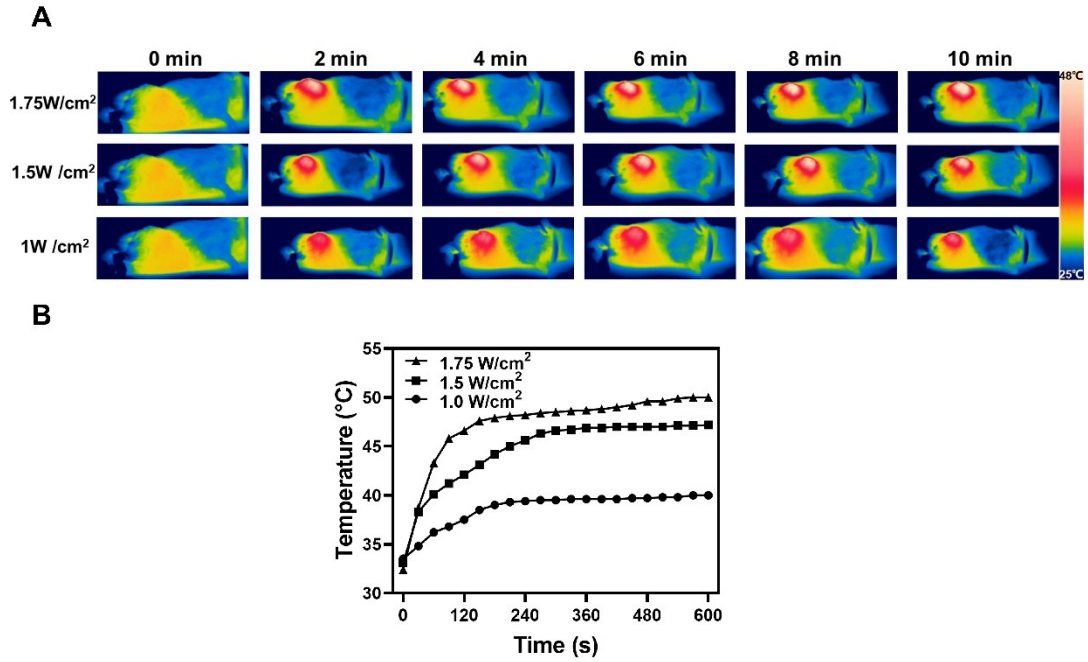


Figure S9. Infrared thermal images of 4T1 subcutaneous tumor-bearing mice treated with Ce6@HMPB NPs under 808 nm laser irradiation with different power (A) and the corresponding temperature changes of tumor (B).

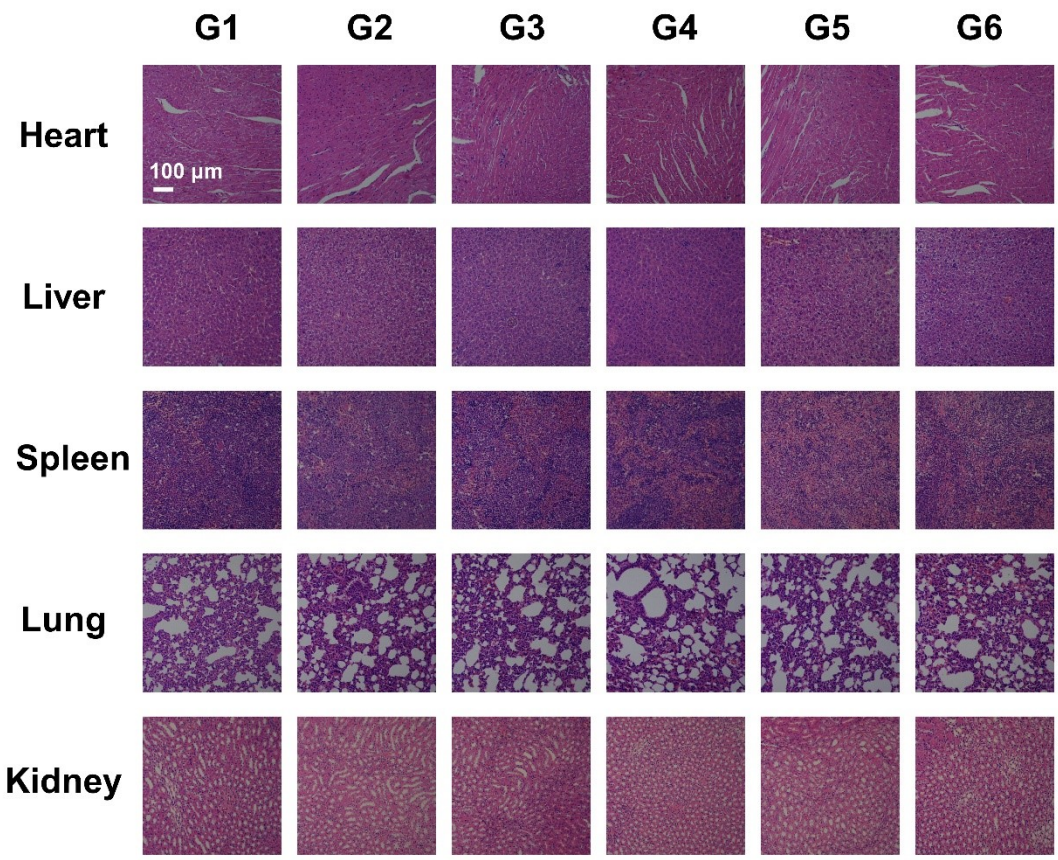


Figure S10. H&E staining images of five major organs (heart, liver, spleen, lung, and kidney) in 4T1 subcutaneous tumor-bearing mice at day 14 in the following groups. G1: Saline, G2: Ce6+660 nm laser, G3: Ce6@HMPB, G4: Ce6@HMPB+808 nm laser, G5: Ce6@HMPB+660 nm laser, G6: Ce6@HMPB+808 nm+660 nm laser. The scale bar is 100 μm.

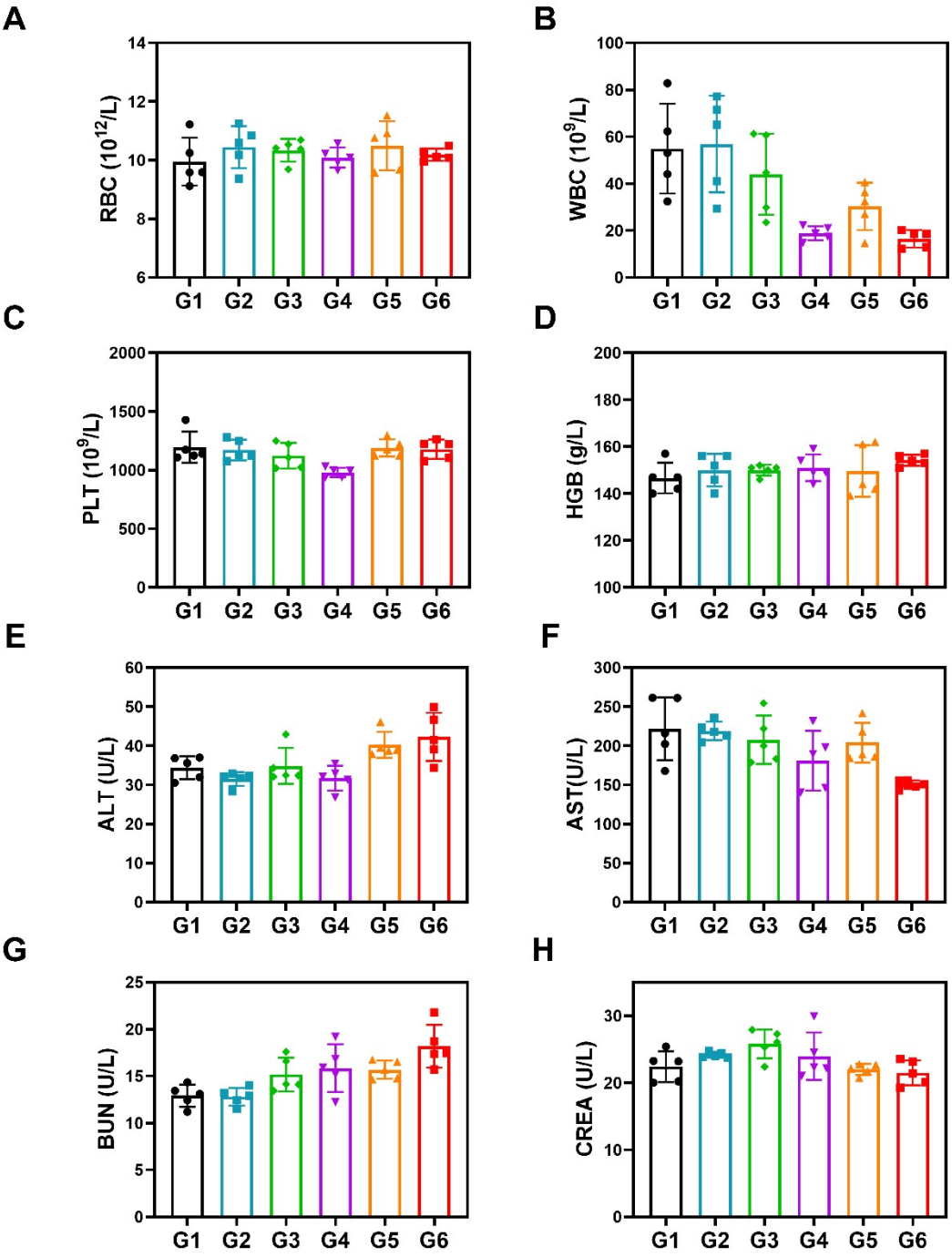


Figure S11. Number of red blood cells (RBC, A), white blood cells (WBC, B), platelets (PLT, C) in blood. Concentration of hemoglobin (HGB, D), alanine transaminase (ALT, E), aspartate transaminase (AST, F), blood urea nitrogen (BUN, G) and creatinine (CREA, H) in serum from blood of mice with different treatment. G1: Saline, G2: Ce6+660 nm laser, G3: Ce6@HMPB, G4: Ce6@HMPB+808 nm laser, G5: Ce6@HMPB+660 nm laser, G6: Ce6@HMPB+808 nm+660 nm laser. Error bar indicates SD (n=5).

Table S1. The diameter, ζ-potential, polydispersity index (PDI) and encapsulation efficiency of Ce6@HMPB NPs at different feeding amout ratio of Ce6 and HMPB NPs.

| **Feeding amout ratio（$m_{Ce6}$:$m_{HMPB\ NPs}$）** | **Z-Average (d.nm)** | **ζ-Potential (mV)** | **PDI** | **Encapsulation Efficiency (%)** |
|---|---|---|---|---|
| **1：10** | 237.2 | -21.4 | 0.138 | 97.45 |
| **2：10** | 251.1 | -19.7 | 0.184 | 98.44 |
| **3：10** | 324.1 | -20.2 | 0.249 | 99.08 |
| **4：10** | 387.3 | -22.7 | 0.395 | 99.25 |

References

1. H. Lin, S. Gao, C. Dai, Y. Chen and J. Shi, *J. Am. Chem. Soc.*, 2017, **139**, 16235-16247.
2. T. Stylianopoulos, J. D. Martin, V. P. Chauhan, S. R. Jain, B. Diop-Frimpong, N. Bardeesy, B. L. Smith, C. R. Ferrone, F. J. Hornicek, Y. Boucher, L. L. Munn and R. K. Jain, *Proc. Natl. Acad. Sci. U. S. A.*, 2012, **109**, 15101-15108.